IEEE Access
Multidisciplinary ⋮ Rapid Review ⋮ Open Access Journal

Received April 7, 2019, accepted April 24, 2019, date of publication April 30, 2019, date of current version May 10, 2019.

Digital Object Identifier 10.1109/ACCESS.2019.2914068

Robust Finite-Time Attitude Tracking Control of a CMG-Based AUV With Unknown Disturbances and Input Saturation

RUIKUN XU[1], GUOYUAN TANG[1,2], LIJUN HAN[1], HUI HUANG[1], AND DE XIE[1,2]
[1]School of Naval Architecture and Ocean Engineering, Huazhong University of Science and Technology, Wuhan 430074, China
[2]Collaborative Innovation Center for Advanced Ship and Deep-Sea Exploration (CISSE), Shanghai 200240, China

Corresponding author: Guoyuan Tang (tgyuan@ hust.edu.cn)

This work was supported in part by the HUST Interdisciplinary Innovation Team Project, in part by the Fundamental Research Funds for the Central Universities under Grant 2018KFYYXJJ012, and in part by the Innovation Foundation of Maritime Defense Technologies Innovation Center.

ABSTRACT This paper focuses on the attitude tracking control of the autonomous underwater vehicle (AUV) using control moment gyros (CMGs) with the lumped nonlinearities including model uncertainty, coupling dynamic property, external disturbance, and input saturation. To describe the attitude of the AUV without singularities, quaternions are used to describe its translational and rotational motion. A finite-time convergent extended state observer (FTCESO) in conjunction with the sliding mode control (SMC) approach is exploited to design the tracking controller for the closed-loop system with the finite-time convergence. Meanwhile, in order to release the burden of the observer, the anti-windup compensator is utilized to handle the nonlinearity of input saturation. A switch function is considered to make a switch between the robust controller and the constant-rate reaching law. Subsequently, with consideration of the inherent singularity problem of actuator dynamics, the constrained steering logic is implemented to avoid this issue without introducing other torque errors in theory. Finite-time stability of the attitude tracking system is guaranteed by the Lyapunov-based approach. Finally, the simulation results validate the attitude tracking performance of the CMG-based AUV with the proposed control strategy, when it is subject to the stated nonlinear uncertainties.

INDEX TERMS Autonomous underwater vehicle, control moment gyros, attitude tracking control, extended state observer, input saturation.

I. INTRODUCTION

To serve the increasing demands on marine resources development and scientific research, underwater robots including AUVs, and remotely operated vehicle (ROVs) are raised to perform diversified tasks in a complex marine environment. In the control literature, researches on three-axis attitude tracking control for AUVs are not common in comparison with other motion control, such as path following [1], [2], target or trajectory tracking [3]–[5], and coordinated formation [6], [7]. As a matter of fact, the process of AUVs executing command tasks is required to realize the control capability, in coordination with the effects of translational and rotational motions. In such cases, attitude maneuver control cannot be neglected due to its basic influence on the operation performance. It is noteworthy that position and attitude tracking control problems for AUVs in six degrees-of-freedom (DOFs) are widely focused on fully actuated configurations [8]–[10]. Meanwhile, attitude control for underactuated AUVs is always based on the decoupling dynamic equations or simplified assumptions of small-angle maneuver to formulate the control scheme in a single direction [11], [12]. By analyzing the preceding literature, it can be used to conclude that for controlling the attitude in a more realistic three-dimensional (3D) manner, it is deserved to make a difference to handle this obstacle. It's well known that CMGs have been widely utilized as angular momentum devices to produce the attitude control torque in the field of aerospace [13]. In terms of its application under the water, CMGs were proposed by Thornton et al. to store energy and to achieve unrestricted attitude control for AUVs [14]. More specifically, AUVs with internal CMG system can generate

The associate editor coordinating the review of this manuscript and approving it for publication was Halil Ersin Soken.

the desired moment with relative fluid motion to maintain the control authority in accordance with a low speed or even zero speed [15], [16]. Seen in this light, CMG-based AUVs are capable of controlling the attitude with a zero radius turning circle and stabilizing the attitude while translating in the surge direction [16].

Although, as stated above, it's predictable that performing precise attitude control for the AUV is an intractable task in a realistic environment with the consideration of modeling uncertainties and unknown time-varying disturbances. To remedy this, a variety of control methods have been recommended to solve the challenging technical problems. Pettersen and Egeland considered the position and attitude stabilization control problem for AUVs with reduced actuators, and a feedback control law was proposed to realize the exponential stabilization [17]. Subsequently, Bartolini and Pisano addressed the black-box position and attitude tracking for a fully actuated AUV via the second-order SMC technique [18]. SMC methods possess the robustness to attenuate the effects of system uncertainties [19], [20], which combined with backstepping design [21], adaptive control [22], neural network (NN) and fuzzy control approach [23], [24], make them more popular in the control engineering. To address planar trajectory tracking control of underactuated AUVs, terminal SMC (TSMC) method was proposed to alleviate the effects of unknown external disturbances caused by ocean currents and waves [25]. To promote the disturbance rejection of SMC methods, an adaptive multiple-input and multiple-output extended-state-observer (MIMO-ESO) was designed in [26] to estimate the unmeasurable velocities and time-varying disturbances.

In regard to the application of SMC technique in the attitude control of AUVs, it also becomes a highlight. By resorting to the decomposed second-order dynamics and small-angle attitude control to simplify the analysis complexity, an adaptive SMC approach was proposed by Cui et al. for designing the attitude control scheme for AUVs with input nonlinearities and external disturbances [12]. Compared with the studies on attitude control for AUVs, it can be viewed that the achievements of spacecraft attitude control were remarkable. In [27], the adaptive law and ESO were employed to formulate the SMC scheme for the attitude tracking control of a spacecraft with inertia uncertainty and external disturbance. In addition, an adaptive non-singular fast TSMC method was designed in [28] for the finite-time convergence when the spacecraft was suffering from external disturbances, actuator faults and saturation. In [29], an integral TSMC was presented for a spacecraft with actuator uncertainties and external disturbances to achieve finite-time attitude tracking. Moreover, for the attitude control problem of a rigid body, Ma et al. proposed an observer-based SMC approach for the transformed dynamics to achieve finite-time stability [30]. Notwithstanding, it should be clarified that attitude tracking control of AUVs needs to take the coupling dynamics from the translational motion into consideration in comparison with the spacecraft. These approaches cannot be directly transplanted to solve the attitude control problem for AUVs, especially when the dynamics of its attitude control device are considered. On the other hand, input saturation problem should be taken into account of the controller design, due to its drawbacks which degrade the system performance or even result in system instability [31]. As a consequence, it's challenging to address 3D attitude tracking control for an AUV with the existence of model uncertainties, time-varying external disturbances and input nonlinearities.

As a supplement, and to the best of the authors' knowledge, there are numbered researchers focused on the study of internal CMG-actuated AUVs. As reported in [16], Thornton investigated the unrestricted attitude stabilization control without considering the external torque disturbances. In [32], the authors utilized a shunting neural dynamical model to address the planar trajectory tracking control of the AUV with CMGs. Subsequently, the authors addressed the large-angle attitude stabilization control of the CMG-actuated AUV with actuator faults [33]. Moreover, based on the backstepping design technique and anti-windup compensator, the authors addressed the problem of 3D trajectory tracking control for a CMG-based AUV with input saturation [34]. Motivated from the aforementioned literature, this paper concentrates on the interesting problem of attitude tracking control for a CMG-actuated AUV under the presence of parameter uncertainties, unknown disturbances and input saturation. In such a scenario, the main contributions of this paper are concluded as follows: (i) attitude tracking control of a CMG-actuated AUV subject to the assumed nonlinear uncertainties is firstly considered in this paper; (ii) a new FTCESO-based SMC approach is constructed for the attitude tracking control to guarantee the finite-time convergence, while among this the anti-windup compensator is employed to handle saturation problem and constrained steering law is taken to control the CMG cluster; (iii) finite-time stability of the proposed control scheme is validated by the Lyapunov stability theory, and the numerical simulations containing two cases demonstrate its effectiveness and reliability.

The reminder of this paper is arranged as follows. Section 2 introduces several useful lemmas to construct a finite-time attitude tracking control scheme; besides, quaternion-based attitude kinematics and the coupled dynamics of a CMG-actuated AUV, together with the control objective are provided. In Section 3, the FTCESO-based sliding mode controller is designed by means of the feedback control technique. Section 4 presents numerical simulations to verify the performance of the proposed controller, and the result analyses are introduced in Section 5. Finally, conclusions and future considerations are drafted in Section 6.

II. PRELIMINARIES AND PROBLEM STATEMENT

A. NOTATION AND LEMMAS

Throughout this paper, following notations are rigorously used. Let $\mathbb{R}$ be the set of real numbers, and $\boldsymbol{I}_n$ be the identity of matrix with the dimension n. For a given vector $\boldsymbol{x} = [x_1, \ldots, x_n]^T \in \mathbb{R}^n$, $\|\boldsymbol{x}\| = \sqrt{\boldsymbol{x}^T\boldsymbol{x}}$ denotes the 2-norm in the

Euclid space; $\text{sig}^{\alpha}(\boldsymbol{x}) = [\text{sgn}(x_1)\,|x_1|^{\alpha}, \ldots, \text{sgn}(x_1)\,|x_n|^{\alpha}]^T$, $|\boldsymbol{x}|^{\alpha} = [|x_1|^{\alpha}, \ldots, |x_n|^{\alpha}]^T$, where $\alpha \in \mathbb{R}$ and $\text{sgn}(\cdot)$ denotes the standard sign function. $\text{diag}[x_1, x_2, \ldots, x_n]$ is a diagonal matrix with scalars $x_1, x_2, \ldots, x_n$.

Lemma 1 [35]: For any $x_1, \cdots, x_n \in \mathbb{R}$, $0 < \rho < 1$, it holds

$$(\sum_{i=1}^{n} |x_i|)^{\rho} \leq \sum_{i=1}^{n} |x_i|^{\rho} \tag{1}$$

Lemma 2 [36]: For any $\iota_1, \iota_2 > 0, 0 < \iota < 1$, if the Lyapunov function V satisfies $\dot{V}(x) + \iota_1 V(x) + \iota_2 V^{\iota}(x) \leq 0$, then V converges to zero in finite-time, and the settling time T_0 is given by

$$T_0 \leq \frac{1}{\iota_1(1-\iota)} \ln \frac{\iota_1 V^{1-\iota}(x_0) + \iota_2}{\iota_2} \tag{2}$$

Lemma 3 [37]: For any $x, \sigma \in \mathbb{R}$, $\varrho > 0$, one has

$$0 \leq \sigma\,|x| - \sigma x \tanh(\chi \sigma x / \varrho) \leq \varrho \tag{3}$$

where $\tanh(\cdot)$ denotes the hyperbolic tangent function and $\chi = e^{-(\chi+1)}$, i.e. $\chi = 0.2785$.

B. MODEL OF A CMG-BASED AUV

Consider the vehicle fixed with the body-fixed frame {B} related to the earth-fixed frame {E}. In order to avoid the singularity problem from the Euler angles in large-angle maneuver, unit parameters are employed to represent the rotational motion which means that $\boldsymbol{q} = [\boldsymbol{\xi}^T, \eta]^T$ denotes the body attitude satisfying the relationship $\boldsymbol{\xi}^T\boldsymbol{\xi} + \eta^2 = 1$, where $\boldsymbol{\xi} = [\xi_1, \xi_2, \xi_3]^T$ shows the vector part and η is a scalar. As a result, attitude kinematics of this vehicle are governed by

$$\begin{cases} \dot{\boldsymbol{\xi}} = \frac{1}{2}(\eta \boldsymbol{I}_3 + \boldsymbol{\xi}^{\times})\boldsymbol{\upsilon}_2 \\ \dot{\eta} = -\frac{1}{2}\boldsymbol{\xi}^T \boldsymbol{\upsilon}_2 \end{cases} \tag{4}$$

where $\boldsymbol{\upsilon}_2 = [p, q, r]^T$ is the angular velocity of the vehicle expressed in the frame {B} and skew matrix $\boldsymbol{\xi}^{\times}$ is defined as following

$$\boldsymbol{\xi}^{\times} = \begin{bmatrix} 0 & -\xi_3 & \xi_2 \\ \xi_3 & 0 & -\xi_1 \\ -\xi_2 & \xi_1 & 0 \end{bmatrix} \tag{5}$$

As presented in [38], the linear velocity transformation of this vehicle from the frame {E} to the frame {B} can be defined by

$$\dot{\boldsymbol{\eta}}_1 = \boldsymbol{E}(\boldsymbol{q})\boldsymbol{\upsilon}_1 \tag{6}$$

where $\boldsymbol{\eta}_1 = [x, y, z]^T$ denotes the vehicle position vector given in the frame {E}, $\boldsymbol{\upsilon}_1 = [u, v, w]^T$ is the linear velocity vector in the frame {B} and matrix $\boldsymbol{E}(\boldsymbol{q})$ is expressed as

$$\boldsymbol{E}(\boldsymbol{q}) = \begin{bmatrix} 1-2(\xi_2^2+\xi_3^2) & 2(\xi_1\xi_2 - \xi_3\eta) & 2(\xi_1\xi_3+\xi_2\eta) \\ 2(\xi_1\xi_2+\xi_3\eta) & 1-2(\xi_1^2+\xi_3^2) & 2(\xi_2\xi_3 - \xi_1\eta) \\ 2(\xi_1\xi_3 - \xi_2\eta) & 2(\xi_2\xi_3+\xi_1\eta) & 1-2(\xi_1^2+\xi_2^2) \end{bmatrix} \tag{7}$$

Different from [16], [34], this paper won't take the assumption that the CMG-based vehicle has coincident centers of gravity and buoyancy to acquire the ability of zero-radius maneuver. To be more specific, the existence of metacentric restoring forces may take trouble to realize the attitude control. Accordingly, the translational and rotational dynamic equations in [34] can be updated as follows

$$\begin{cases} m(\dot{\boldsymbol{\upsilon}}_1 + \boldsymbol{\upsilon}_2 \times \boldsymbol{\upsilon}_1) = \boldsymbol{\tau}_1 \\ \boldsymbol{I}\dot{\boldsymbol{\upsilon}}_2 + \dot{\boldsymbol{H}} + \boldsymbol{\upsilon}_2 \times (\boldsymbol{I}\boldsymbol{\upsilon}_2 + \boldsymbol{H}) = \boldsymbol{\tau}_2 + \boldsymbol{d} \end{cases} \tag{8}$$

where m stands for the total mass of the vehicle; $\boldsymbol{I} = \text{diag}[I_x, I_y, I_z]$ represents the inertia matrix; $\boldsymbol{H} = [H_x, H_y, H_z]^T$ denotes the angular momentum generated from the CMG system which will be given later; $\boldsymbol{d}$ is the unknown bounded disturbance vector; $\boldsymbol{\tau}_1 = [X, Y, Z]^T$ and $\boldsymbol{\tau}_2 = [K, M, N]^T$ are the hydrodynamic functions, which are presented as follows

$$\begin{cases} X = X_{\dot{u}}\dot{u} + X_{u|u|}u\,|u| + X_{q|q|}q^2 + X_{r|r|}r^2 + X_{vr}vr \\ \qquad +X_{wq}wq + \tau_u \\ Y = Y_{\dot{v}}\dot{v} + Y_{\dot{r}}\dot{r} + Y_{v|v|}v\,|v| + Y_{r|r|}r|r| + Y_{uv}uv + Y_{ur}ur \\ \qquad +Y_{wp}wp + Y_{pq}pq \\ Z = Z_{\dot{w}}\dot{w} + Z_{\dot{q}}\dot{q} + Z_{uw}uw + Z_{w|w|}w\,|w| + Z_{q|q|}q\,|q| \\ \qquad +Z_{uq}uq + Z_{vp}vp + Z_{rp}rp \end{cases} \tag{9}$$

and

$$\begin{cases} K = K_{\dot{p}}\dot{p} + K_{p|p|}p\,|p| - mgh\cos\theta\sin\phi \\ M = M_{\dot{w}}\dot{w} + M_{\dot{q}}\dot{q} + M_{w|w|}w\,|w| + M_{q|q|}q\,|q| + M_{uq}uq \\ \qquad ; +M_{vp}vp + M_{rp}rp - mgh\sin\theta \\ N = N_{\dot{v}}\dot{v} + N_{\dot{r}}\dot{r} + N_{uv}uv + N_{v|v|}v\,|v| + N_{r|r|}r\,|r| \\ \qquad +N_{wp}wp + N_{ur}ur \end{cases} \tag{10}$$

where τ_u is the control force provided by the propulsion system; $X_{(\cdot)}$, $Y_{(\cdot)}$, $Z_{(\cdot)}$, $K_{(\cdot)}$, $M_{(\cdot)}$ and $N_{(\cdot)}$ are the corresponding hydrodynamic parameters; $g = 9.8\ ms^2$ denotes the acceleration of gravity and $h = 0.02$ m is the metacentric height. Denote ϕ, θ and ψ as the actual roll angle, pitch angle and yaw angle of the vehicle, respectively, and then one can obtain the relationship between Euler angles and unit parameters [38]

$$\begin{cases} \theta = -\arcsin(E_{31}), \quad \theta \neq \pi/2 \\ \phi = atan2(E_{32}, E_{33}) \\ \psi = atan2(E_{21}, E_{11}) \end{cases} \tag{11}$$

where E_{ij} denotes the i-th row and j-th column element of matrix $\boldsymbol{E}(\boldsymbol{q})$ and the function $\text{atan2}(\cdot,\cdot)$ represents the arctangent function with two arguments which ensures the result belongs to $(-\pi, \pi]$.

Remark 1: Similar to [12], the thrust force τ_u is considered to be a constant when this vehicle is implementing the task of attitude tracking using CMGs. Yet, this paper won't take the assumption of small-angle attitude maneuver and will control the vehicle's three-axis attitude in 3D space.

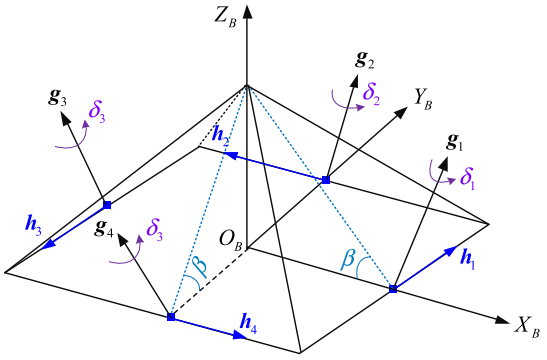

FIGURE 1. Pyramid-type CMGs.

Remark 2: As shown in (9) and (10), it should be claimed that the actual inertia matrix of this system in 6 DOFs is not a diagonal matrix, which means that the vehicle is coupled with control inputs to directly affect its' translational and rotational motion, and this may cause the trouble in the tracking mission.

As introduced in [34], pyramid-type CMG system is considered as the internal attitude control device to produce the control torque and its basic structure is shown in Fig. 1.

As depicted in Fig. 1, $\{O_B X_B Y_B\}$ denotes the body-fixed frame $\{\mathrm{B}\}$. $\beta = \cos^{-1}(1/\sqrt{3})$ is the skew angle; $\boldsymbol{g}_i$ denotes the i-th gimbal axis vector and the i-th momentum axis vector $\boldsymbol{h}_i$ can be expressed as the function of its gimbal angle δ_i. Therefore, the total angular momentum $\boldsymbol{H}$ can be defined by

$$\boldsymbol{H} = \sum_{i=1}^{4} \boldsymbol{h}_i(\delta_i) = J_0 \begin{bmatrix} -c\beta s\delta_1 - c\delta_2 + c\beta s\delta_3 + c\delta_4 \\ c\delta_1 - c\beta s\delta_2 - c\delta_3 + c\beta s\delta_4 \\ s\beta(s\delta_1 + s\delta_2 + s\delta_3 + s\delta_4) \end{bmatrix} \tag{12}$$

where $c\cdot = \cos(\cdot)$, $s\cdot = \sin(\cdot)$ and scalar J_0 is the nominal magnitude of angular momentum of each gyro.

Consider the fact that output torque of the CMG system is derived from the variation of its angular momentum [39], while the two directions are opposite, which means that

$$\boldsymbol{\tau} = -\dot{\boldsymbol{H}} = -J_0 \boldsymbol{C}\dot{\boldsymbol{\delta}} \tag{13}$$

where $\boldsymbol{\tau} = [\tau_p, \tau_q, \tau_r]^T$ represents the output torque, $\dot{\boldsymbol{\delta}} = [\dot{\delta}_1, \dot{\delta}_2, \dot{\delta}_3, \dot{\delta}_4]^T$ is the gimbal rate vector and Jacobian matrix $\boldsymbol{C}$ of the CMG system is calculated as

$$\boldsymbol{C} = \begin{bmatrix} -c\beta c\delta_1 & s\delta_2 & c\beta c\delta_3 & -s\delta_4 \\ -s\delta_1 & -c\beta c\delta_2 & s\delta_3 & c\beta c\delta_4 \\ s\beta c\delta_1 & s\beta c\delta_2 & s\beta c\delta_3 & s\beta c\delta_4 \end{bmatrix} \tag{14}$$

To incorporate practical considerations of the capability of the CMG system for torque output, the input saturation problem needs to be taken into account of the controller design. Hence, to cater to this notion, using the saturation function $\mathrm{sat}(\boldsymbol{\tau}) = \boldsymbol{\tau}_d + \Delta\boldsymbol{\tau}$ in the forthcoming controller design, where $\boldsymbol{\tau}_d = [\tau_{dp}, \tau_{dq}, \tau_{dr}]^T$ is the desired input vector, $\mathrm{sat}(\boldsymbol{\tau}) = [\mathrm{sat}(\tau_p), \mathrm{sat}(\tau_q), \mathrm{sat}(\tau_r)]^T$ and $\mathrm{sat}(\cdot)$ is defined as

$$sat(\tau_\kappa) = \begin{cases} \bar{\tau}_\kappa sign(\tau_\kappa), & |\tau_{d\kappa}| \geq \bar{\tau}_\kappa \\ \tau_\kappa, & |\tau_{d\kappa}| < \bar{\tau}_\kappa \end{cases} \tag{15}$$

where $\kappa \in \Omega\{p, q, r\}$, $\bar{\tau}_\kappa$ denotes the assumed maximum control torque, which is less than the actual maximum output torque of the CMG system. In addition, one can get the saturation error vector $\Delta\boldsymbol{\tau} = [\Delta\tau_p, \Delta\tau_q, \Delta\tau_r]^T$, where $\Delta\tau_\kappa = \mathrm{sat}(\tau_k) - \tau_{d\kappa}, \kappa \in \Omega$.

C. PROBLEM FORMULATION

Consider the CMG-based AUV with the attitude kinematics given in (4), the position kinematics and dynamics shown in (8), together with the kinematics of the CMG system. In the sequel, denote $\boldsymbol{q}_d = [\boldsymbol{\xi}_d^T, \eta_d]^T$ as the expected vehicle attitude with its vector part $\boldsymbol{\xi}_d = [\xi_{1d}, \xi_{2d}, \xi_{3d}]^T$ satisfying $\|\boldsymbol{q}_d\| = 1$, and the desired attitude trajectory is derived from

$$\begin{cases} \dot{\boldsymbol{\xi}}_d = \frac{1}{2}(\eta_d \boldsymbol{I}_3 + \boldsymbol{\xi}_d^\times)\boldsymbol{\upsilon}_d \\ \dot{\eta}_d = -\frac{1}{2}\boldsymbol{\xi}_d^T \boldsymbol{\upsilon}_d \end{cases} \tag{16}$$

where $\boldsymbol{\upsilon}_d = [p_d, q_d, r_d]^T$ represents the desired angular velocity. Subsequently, the attitude error kinematics are generated as [10]

$$\begin{cases} \dot{\boldsymbol{\xi}}_e = \frac{1}{2}(\eta_e \boldsymbol{I}_3 + \boldsymbol{\xi}_e^\times)\boldsymbol{\upsilon}_e \\ \dot{\eta}_e = -\frac{1}{2}\boldsymbol{\xi}_e^T \boldsymbol{\upsilon}_e \end{cases} \tag{17}$$

where $\boldsymbol{\upsilon}_e = \boldsymbol{\upsilon}_2 - \boldsymbol{\upsilon}_d = [p_e, q_e, r_e]^T$, and the attitude error variables $\boldsymbol{\xi}_e = [\xi_{1e}, \xi_{2e}, \xi_{3e}]^T$ and η_e are calculated as the following form of a block matrix [40]

$$\boldsymbol{q}_e = \begin{bmatrix} \eta_d \boldsymbol{I}_3 - \boldsymbol{\xi}_d^\times & -\boldsymbol{\xi}_d \\ \boldsymbol{\xi}_d^T & \eta_d \end{bmatrix} \boldsymbol{q} \tag{18}$$

with $\boldsymbol{q}_e = [\boldsymbol{\xi}_e^T, \eta_e]^T$. Here, it should be noted that $\boldsymbol{\xi}_e = \boldsymbol{0} \in \mathbb{R}^3$ and $\eta_e = \pm 1$ represent two equilibrium points with the attachment of the same physical point [18].

To develop the control scheme in a more realistic scenario, following assumptions are put forward to formulate the control objective.

Assumption 1: In the kinematic and dynamic equations of this vehicle as shown in (8), full states can be measured, which indicates that linear and angular velocity vector $\boldsymbol{\upsilon}_1$, $\boldsymbol{\upsilon}_2$ can be acquired. Also, the unit quaternion $\boldsymbol{q}$, gimbal rate $\boldsymbol{\delta}$ and gimbal angle $\dot{\boldsymbol{\delta}}$ of the CMG system are available in the design of feedback controller.

Assumption 2: As motivated from practice, nominal model parameters are taken into the controller development to consider the system with parametric uncertainties. Meanwhile, this vehicle is assumed to expose to the unknown bounded disturbances.

Motivated by the above considerations, the target of this paper is then to develop a robust feedback controller to stabilize the resulting attitude control system (17) in a finite time, despite of the parameter uncertainties, external disturbances and input saturation.

III. ATTITUDE TRACKING CONTROLLER DESIGN

As shown in Fig. 2, a block diagram of the attitude tracking control system is presented to lead the controller design. From the structural topology, it can be observed that the

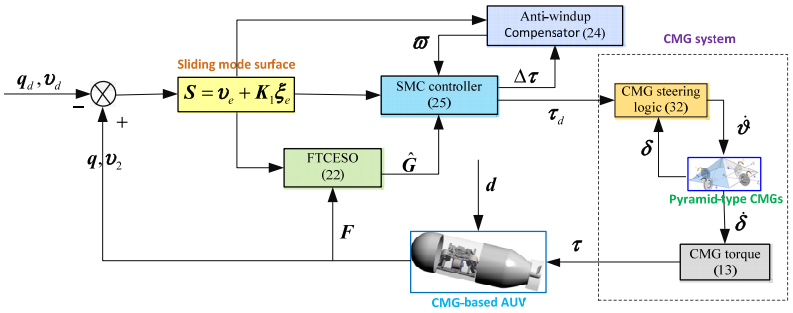

FIGURE 2. Structure of the FTCESO-based sliding model controller.

developed controller is twofold. In fact, the first is observed-based sliding-mode controller design and the second is the steering law for the pyramid-type CMG system.

A. FTCESO-BASED SLIDING-MODE CONTROLLER DESIGN

First, construct the following common linear sliding mode manifold

$$\boldsymbol{S} = \boldsymbol{v}_e + \boldsymbol{K}_1\boldsymbol{\xi}_e \tag{19}$$

where $\boldsymbol{K}_1$ is a symmetric positive matrix.

As stated above, the finite-time attitude tracking controller should be designed without resorting to the exact knowledge of modeling parameters and despite of the presence of undesired disturbances and input saturation. Hence, the inertia matrix and known hydrodynamic parameters are not precise to result in $\boldsymbol{I} = \boldsymbol{I}_0 + \Delta\boldsymbol{I}$, $\boldsymbol{\tau}_2 = \boldsymbol{\tau}_2^0 + \Delta\boldsymbol{\tau}_2$, where $\boldsymbol{I}_0$ and $\boldsymbol{\tau}_2^0$ denote relative values from the nominal model; $\Delta\boldsymbol{I}$ and $\Delta\boldsymbol{\tau}_2$ are the unmodeled parts. Subsequently, using (17) and (19), rotational dynamics can be simplified to

$$\begin{aligned}\dot{\boldsymbol{S}} &= \dot{\boldsymbol{v}}_e + \boldsymbol{K}_1\dot{\boldsymbol{\xi}}_e \\ &= \boldsymbol{I}_0^{-1}[\boldsymbol{\tau}_2^0 - \boldsymbol{v}_2 \times (\boldsymbol{I}_0\boldsymbol{v}_2 + \boldsymbol{H}) + \frac{1}{2}\boldsymbol{I}_0\boldsymbol{K}_1(\eta_e\boldsymbol{I}_3 + \boldsymbol{\xi}_e^{\times})\boldsymbol{v}_e \\ &\quad -\boldsymbol{I}_0\dot{\boldsymbol{v}}_d + \boldsymbol{d} + \Delta\boldsymbol{\tau}_2 - \Delta\dot{\boldsymbol{I}}\upsilon_2 - \boldsymbol{v}_2 \times \Delta\boldsymbol{I}\boldsymbol{v}_2 + \boldsymbol{\tau}_d + \Delta\boldsymbol{\tau}] \\ &= \boldsymbol{F} + \boldsymbol{G} + \boldsymbol{I}_0^{-1}(\boldsymbol{\tau}_d + \Delta\boldsymbol{\tau})\end{aligned} \tag{20}$$

where the known hydrodynamic function $\boldsymbol{F}$ and uncertain function $\boldsymbol{G}$ are given by

$$\begin{cases}\boldsymbol{F} = \boldsymbol{I}_0^{-1}[\boldsymbol{\tau}_2^0 - \boldsymbol{I}_0\dot{\boldsymbol{v}}_d - \boldsymbol{v}_2 \times (\boldsymbol{I}_0\boldsymbol{v}_2 + \boldsymbol{H}) \\ \qquad\quad +\frac{1}{2}\boldsymbol{I}_0\boldsymbol{K}_1(\eta_e\boldsymbol{I}_3 + \boldsymbol{\xi}_e^{\times})\boldsymbol{v}_e] \\ \boldsymbol{G} = \boldsymbol{I}_0^{-1}(\boldsymbol{d} + \Delta\boldsymbol{\tau}_2 - \Delta\boldsymbol{I}\dot{\boldsymbol{v}}_2 - \boldsymbol{v}_2 \times \Delta\boldsymbol{I}\boldsymbol{v}_2)\end{cases} \tag{21}$$

where $\boldsymbol{G}$ contains the multisource unknown uncertainties, i.e., time-varying external disturbances (caused by the wind, wave and current), uncertain modeling parameters, time-varying inertia parametric uncertainties (considered from the practical perspective).

Motivated by the work in [41], the following FTCESO is proposed for the sake of achieving finite-time stabilization of the attitude error system

$$\begin{cases}\tilde{\boldsymbol{S}} = \boldsymbol{S} - \hat{\boldsymbol{S}} \\ \dot{\hat{\boldsymbol{S}}} = \boldsymbol{I}_0^{-1}\boldsymbol{\tau}_d + \boldsymbol{F} + \hat{\boldsymbol{G}} + \gamma_1(\mathrm{sig}^{\alpha_1}(\tilde{\boldsymbol{S}}) + \mathrm{sig}^{\beta_1}(\tilde{\boldsymbol{S}})) + \gamma_2\mathrm{sgmf}(\tilde{\boldsymbol{S}}) \\ \dot{\hat{\boldsymbol{G}}} = \gamma_3(\mathrm{sig}^{\alpha_2}(\tilde{\boldsymbol{S}}) + \mathrm{sig}^{\beta_2}(\tilde{\boldsymbol{S}})) + \gamma_4\mathrm{sgmf}(\tilde{\boldsymbol{S}})\end{cases} \tag{22}$$

where $0.5 < \alpha_1 < 1$, $\alpha_2 = 2\alpha_1 - 1$, $\beta_1 = 1\alpha_1$, $\beta_2 = \beta_1 + 1/\beta_1 - 1$, $\gamma_i > 1, i = 1, 2, 3, 4$; $\tilde{\boldsymbol{S}} = [\tilde{S}_1, \tilde{S}_2, \tilde{S}_3]^T$ is the observation error; $\hat{\boldsymbol{S}}$ and $\hat{\boldsymbol{G}}$ represent the estimations of $\boldsymbol{S}$ and $\boldsymbol{G}$, respectively; in addition, the function $\mathrm{sgmf}(\tilde{\boldsymbol{S}}) = [\mathrm{sgmf}(\tilde{S}_1), \mathrm{sgmf}(\tilde{S}_2), \mathrm{sgmf}(\tilde{S}_3)]^T$ is defined as

$$\mathrm{sgmf}(\tilde{S}_i) = \begin{cases}2\left(\frac{1}{1+\exp(-\lambda_1\tilde{S}_i)} - \frac{1}{2}\right), & |\tilde{S}_i| \le \lambda_2 \\ \mathrm{sign}(\tilde{S}_i), & |\tilde{S}_i| > \lambda_2\end{cases} \tag{23}$$

where $\lambda_1, \lambda_2 > 0, i = 1, 2, 3$.

Subsequently, note the fact that the CMG-based vehicle is subject to input saturation. To handle this obstacle, and also to alleviate the burden of designed observer, the anti-windup compensator is constructed as

$$\dot{\boldsymbol{\varpi}} = \begin{cases}0, & \|\boldsymbol{\varpi}\| \le \varpi \\ -c_1\boldsymbol{\varpi} - c_2\mathrm{sig}^c(\boldsymbol{\varpi}) - \frac{\left\|\boldsymbol{S}^T\boldsymbol{I}_0^{-1}\Delta\boldsymbol{\tau}\right\| + 12\Delta\boldsymbol{\tau}^T\Delta\boldsymbol{\tau}}{\|\boldsymbol{\varpi}\|^2}\boldsymbol{\varpi} \\ +\Delta\boldsymbol{\tau}, & \|\boldsymbol{\varpi}\| > \varpi\end{cases} \tag{24}$$

where $c_1, c_2 > 0$, $0 < c < 1$, ϖ is a small positive constant. As a consequence, the desired control torque for the CMG system is formulated as

$$\boldsymbol{\tau}_d = -\boldsymbol{I}_0(\boldsymbol{F} + \mathrm{sf}(t)(\hat{\boldsymbol{G}} + \boldsymbol{\tau}_\delta) + \boldsymbol{\tau}_r + k_4\boldsymbol{\varpi}) \tag{25}$$

where $k_i > 0$, $i = 1, 2, 3, 4$, and the reaching law $\boldsymbol{\tau}_r$ is defined as

$$\boldsymbol{\tau}_r = k_1\boldsymbol{S} + k_2(1 - \mathrm{sf}(t)(\mathrm{t}))\mathrm{sign}(\boldsymbol{S}) + k_3\mathrm{sig}^c(\boldsymbol{S}) \tag{26}$$

In addition, assume that sliding surface $\boldsymbol{S}$ is with the component form $\boldsymbol{S} = [S_1, S_2, S_3]^T$ and then the robust term $\boldsymbol{\tau}_\delta = [\tau_{\delta 1}, \tau_{\delta 2}, \tau_{\delta 3}]^T$ can be presented as [42]

$$\tau_{\delta i} = \sigma\tanh(\sigma\chi S_i/\varrho), \quad i = 1, 2, 3 \tag{27}$$

where $\chi = 0.2785$, $\varrho > 0$, $\sigma > \Lambda$ and the concept of Λ will be given later; $sf(t)$ is a switch function, governed by

$$\mathrm{sf}(t)(\mathrm{t}) = \begin{cases} 1, & \left\|\hat{\boldsymbol{G}}\right\| \geq G_M \\ 0, & \left\|\hat{\boldsymbol{G}}\right\| \leq G_M \end{cases} \tag{28}$$

where G_M is a positive constant. Note that relative variables presented in uncertain function $\boldsymbol{G}$ are bounded in practice, and thus we can assume that $\|\boldsymbol{G}_d\| \leq G_M$, where $\boldsymbol{G}_d$ is the desired nonlinear function of $\boldsymbol{G}$, when the system converges to its desired trajectory.

Remark 3: In terms of the CMGs, the designed control input $\boldsymbol{\tau}_d$ is actually the desired output torque. Meanwhile, the CMG output torque $\boldsymbol{\tau}$ will be generated from its kinematics (13), and the attitude tracking control system should possess the robust stability to cancel the effects of the control torque errors, which can be considered as a part of the uncertain function $\boldsymbol{G}$.

B. STEERING LAW FOR THE CMG SYSTEM

Before proceeding further, it can be proven that the Jacobian matrix $\boldsymbol{C}$ in (13) may not be of full rank due to the fact that $\boldsymbol{C} \in \mathbb{R}^{3\times 4}$ is time-varying with the variation of the gimbal rate vector $\dot{\boldsymbol{\delta}}$. In fact, pseudo inverse matrix of $\boldsymbol{C}$ may not exist when the CMG system comes into a singular configuration where the CMG system cannot produce the torque along the direction of its commanded torque, and the singular measure is defined as $D = \det(\boldsymbol{C}^T\boldsymbol{C})$ [40]. In light of that, various steering laws were designed to avoid the singular configuration or escape from the unavoidable singularities [43], [44].

In order to reduce the control torque errors as much as possible, constrained steering law is utilized to produce exact and strictly real-time control torque [45]. The idea of this method is using the algebraic constraint of the gimbal angle, like $\delta_1 - \delta_2 + \delta_3 - \delta_4 = 0$, to limit the work space of the CMG system to avoid the singularity problem.

For the sake of convenient description, using vector $\boldsymbol{\vartheta} = [\vartheta_1, \vartheta_2, \vartheta_3]^T$ to simplify the defined constraint, and then the total angular momentum in (12) is updated as

$$\hat{\boldsymbol{H}} = J_0 \begin{bmatrix} s\vartheta_1 s\vartheta_3 - c\beta c\vartheta_1 s\vartheta_2 \\ -s\vartheta_1 s\vartheta_2 - c\beta c\vartheta_1 s\vartheta_3 \\ s\beta s\vartheta_1 (c\vartheta_2 + c\vartheta_3) \end{bmatrix} \tag{29}$$

and correspondingly the Jacobian matrix (14) becomes

$$\hat{\boldsymbol{C}} = \begin{bmatrix} c\beta s\vartheta_1 s\vartheta_2 + c\vartheta_2 s\vartheta_3 & -c\beta c\vartheta_1 c\vartheta_2 & s\vartheta_1 c\vartheta_3 \\ c\beta s\vartheta_1 s\vartheta_3 - c\vartheta_1 s\vartheta_2 & -s\vartheta_1 c\vartheta_2 & -c\beta c\vartheta_1 c\vartheta_3 \\ s\beta c\vartheta_1 (c\vartheta_2 + c\vartheta_3) & -s\beta s\vartheta_1 s\vartheta_2 & -s\beta s\vartheta_1 s\vartheta_3 \end{bmatrix} \tag{30}$$

In accordance with the above considerations, the pyramid-type CMG system will not come into a singular configuration, which means that the updated Jacobian matrix $\hat{\boldsymbol{C}}$ will be of full rank when its angular momentum is inside the restricted workspace [45]. Therefore, from the equation (13), one can get $\hat{\boldsymbol{\vartheta}} = -(J_0\hat{\boldsymbol{C}})^{-1}\boldsymbol{\tau}_d$.

Notwithstanding, the given algebraic constraint of the gimbal angle may not be guaranteed in real situations due to the variation of the gimbal rate. Hence, to avoid this problem, null motion vector is introduced as

$$\boldsymbol{\delta}_n = [(\boldsymbol{c}_2, \boldsymbol{c}_3, \boldsymbol{c}_4), -(\boldsymbol{c}_3, \boldsymbol{c}_4, \boldsymbol{c}_1), (\boldsymbol{c}_4, \boldsymbol{c}_1, \boldsymbol{c}_2), -(\boldsymbol{c}_1, \boldsymbol{c}_2, \boldsymbol{c}_3)]^T \tag{31}$$

where $(\boldsymbol{c}_i, \boldsymbol{c}_j, \boldsymbol{c}_k)$ represents the box product of three vectors $\boldsymbol{c}_i$, $\boldsymbol{c}_j$and $\boldsymbol{c}_k$; $\boldsymbol{c}_i (1 \leq i \leq 4)$ is the i-th column vector of the original Jacobian matrix $\boldsymbol{C}$. It should be pointed out that null motion of the CMG system won't change its angular momentum, which signifies that the output torque will not change as well. In light of that, for the designed control input $\boldsymbol{\tau}_d$ in (25), feedback control law for the CMG system is constructed as

$$\dot{\boldsymbol{\delta}} = \boldsymbol{\Theta}\dot{\boldsymbol{\vartheta}} + k_n\boldsymbol{\delta}_n \tag{32}$$

with $k_n = -\lambda \Big/ \|\boldsymbol{\delta}_n\|^2(\delta_1 - \delta_2 + \delta_3 - \delta_4)(\delta_{n1} - \delta_{n2} + \delta_{n3} - \delta_{n4})$, where λ is a positive feedback constant, δ_{ni} $(1 \leq i \leq 4)$ is the i-th component of vector $\boldsymbol{\delta}_n$, and matrix $\boldsymbol{\Theta}$ is given by

$$\boldsymbol{\Theta} = \begin{bmatrix} 1 & 1 & 0 \\ 1 & 0 & 1 \\ 1 & -1 & 0 \\ 1 & 0 & -1 \end{bmatrix} \tag{33}$$

Remark 4: The achievement of using constrained steering logic for the CMG system to control the AUV's attitude can be shown in [16], [34]; however, it cannot deny the fact that although this method can realize exact and real-time torque output in theory, torque errors in the transformation cannot be stabilized to zero whether in the simulation or actual situations. As a result, the designed control strategy should take this into account to address the internal disturbances.

C. LYAPUNOV-BASED STABILITY ANALYSIS

To inspect finite-time stabiliztation of the error system in (17) actuated by the proposed controller in (25) and (32), several theorems are provided to facilitate the stability analysis.

Theorem 1: Consider the sliding-mode surface defined in (19), and it can be proved that if $\boldsymbol{S}$ approaches zero, i.e. $\lim_{t\to\infty} \boldsymbol{S} = \boldsymbol{0}$, then one has

$$\lim_{t\to\infty} \boldsymbol{\xi}_e = \boldsymbol{0}, \quad \lim_{t\to\infty} \boldsymbol{v}_e = \boldsymbol{0} \tag{34}$$

Proof of Theorem 1 can be found in [46].

Theorem 2: For the dynamic system of the given sliding-mode surface in (20), (21) and FTCESO in (22), error dynamics of the observer can be obtained as follows

$$\begin{cases} \dot{\tilde{\boldsymbol{S}}} = \tilde{\boldsymbol{G}} - \gamma_1(\mathrm{sig}^{\alpha_1}(\tilde{\boldsymbol{S}}) + \mathrm{sig}^{\beta_1}(\tilde{\boldsymbol{S}})) - \gamma_2\mathrm{sgmf}(\tilde{\boldsymbol{S}}) \\ \dot{\tilde{\boldsymbol{G}}} = \boldsymbol{g}(t) - \gamma_3(\mathrm{sig}^{\alpha_1}(\tilde{\boldsymbol{S}}) + \mathrm{sig}^{\beta_1}(\tilde{\boldsymbol{S}})) - \gamma_4\mathrm{sgmf}(\tilde{\boldsymbol{S}}) \end{cases} \tag{35}$$

where $\boldsymbol{g}(t) \triangleq \dot{\boldsymbol{G}}$, $\tilde{\boldsymbol{G}} = \boldsymbol{G} - \hat{\boldsymbol{G}}$. It can be demonstrated that $\tilde{\boldsymbol{S}}$ and $\tilde{\boldsymbol{G}}$ will converge to a residual set Ξ governed by

$$\Xi = \left\{ (\tilde{\boldsymbol{S}}, \tilde{\boldsymbol{G}}) \middle| \left\|\tilde{\boldsymbol{S}}\right\| \leq \Lambda, \left\|\tilde{\boldsymbol{G}}\right\| \leq \Lambda \right\} \tag{36}$$

in finite time, and the convergence time is governed by the observer parameter selection.

Proof of Theorem 2 can be found in [41].

Theorem 3: Consider the CMG-based AUV attitude tracking system described by (4), (8), with the existence of parameter uncertainties, external disturbances and input saturation, satisfying Assumptions 1-2. The control torque is provided by (25), and the steering law for the CMG system is given by (32). For an appropriate control force τ_u with the following parameter conditions

$$\begin{cases} k_1 - 1/2 > 0 \\ c_1 - 1/2 - 1/2k_4^2 > 0 \end{cases} \tag{37}$$

and then finite-time stability of the control system can be achieved.

Proof: Construct the following Lyapunov function

$$V = \frac{1}{2}\boldsymbol{S}^T\boldsymbol{S} + \frac{1}{2}\boldsymbol{\varpi}^T\boldsymbol{\varpi} \tag{38}$$

Differentiating the defined Lyapunov function in (38) with respect to time, and then utilizing (20), (25), (26) yields

$$\begin{aligned} \dot{V} =& \boldsymbol{S}^T[\boldsymbol{F}+\boldsymbol{G}+\boldsymbol{I}_0^{-1}(\boldsymbol{\tau}_d+\Delta\boldsymbol{\tau})]+\boldsymbol{\varpi}^T\dot{\boldsymbol{\varpi}} \\ =& -k_1\boldsymbol{S}^T\boldsymbol{S}-(1-\mathrm{sf}(t)(\mathrm{t}))(\boldsymbol{S}^T\boldsymbol{G}-k_2\sum_{i=1}^{3}|S_i|)-k_3\boldsymbol{S}^T\mathrm{sig}^c(\boldsymbol{S}) \\ & -k_4\boldsymbol{S}^T\boldsymbol{\varpi}+\boldsymbol{S}^T\boldsymbol{I}_0^{-1}\Delta\boldsymbol{\tau}+sf(\mathrm{t})(\boldsymbol{S}^T\tilde{\boldsymbol{G}}-\boldsymbol{S}^T\boldsymbol{\tau}_\delta)+\boldsymbol{\varpi}^T\dot{\boldsymbol{\varpi}} \end{aligned} \tag{39}$$

As stated in Theorem 2, if the observer parameters are selected appropriately, one can obtain $\left\|\tilde{\boldsymbol{G}}\right\| \le \Lambda$ in finite time with $\tilde{\boldsymbol{G}} = [\tilde{G}_1, \tilde{G}_2, \tilde{G}_3]^T$ and $\left|\tilde{G}_i\right| \le \Lambda$, $i = 1, 2, 3$. Then using Lemma 3 and (27) leads to

$$\boldsymbol{S}^T\tilde{\boldsymbol{G}}-\boldsymbol{S}^T\boldsymbol{\tau}_\delta \le \sum_{i=1}^{3}(\sigma\,|S_i|-\sigma S_i\tanh(\chi\sigma S_i/\varrho)) \le 3\varrho \tag{40}$$

In this condition, we know that when $\boldsymbol{G}$ converges to its desired value $\boldsymbol{G}_d$ and $G_M \le k_2$, it holds

$$\boldsymbol{S}^T\boldsymbol{G}_d - k_2\sum_{i=1}^{3}|S_i| \le (G_M - k_2)\sum_{i=1}^{3}|S_i| \le 0 \tag{41}$$

Meanwhile, consider the control system is subject to the input saturation, namely $\|\boldsymbol{\varpi}\| > \varpi$, and we have

$$\begin{aligned} \boldsymbol{\varpi}^T\dot{\boldsymbol{\varpi}} =& -c_1\boldsymbol{\varpi}^T\boldsymbol{\varpi} - c_2\boldsymbol{\varpi}^T\mathrm{sig}^c(\boldsymbol{\varpi}) \\ & - \frac{\left\|\boldsymbol{S}^T\boldsymbol{I}_0^{-1}\Delta\boldsymbol{\tau}\right\| + 1/2\Delta\boldsymbol{\tau}^T\Delta\boldsymbol{\tau}}{\|\boldsymbol{\varpi}\|^2}\boldsymbol{\varpi}^T\boldsymbol{\varpi} + \boldsymbol{\varpi}^T\Delta\boldsymbol{\tau} \end{aligned} \tag{42}$$

Using the following inequalities

$$\begin{cases} -k_4\boldsymbol{S}^T\boldsymbol{\varpi} \le 1/2\boldsymbol{S}^T\boldsymbol{S} + 1/2k_4^2\boldsymbol{\varpi}^T\boldsymbol{\varpi} \\ \boldsymbol{\varpi}^T\Delta\boldsymbol{\tau} \le 1/2\boldsymbol{\varpi}^T\boldsymbol{\varpi} + 1/2\Delta\boldsymbol{\tau}^T\Delta\boldsymbol{\tau} \end{cases} \tag{43}$$

Subsequently, noting the boundary value of $sf(\mathrm{t})$ and then substituting (40), (41), (42)and (43) into (39) yields

$$\begin{aligned} \dot{V} \le& -(k_1 - 1/2)\boldsymbol{S}^T\boldsymbol{S} - k_3\boldsymbol{S}^T\mathrm{sig}^c(\boldsymbol{S}) + 3\varrho \\ & -(c_1 - 1/2 - 1/2k_4^2)\boldsymbol{\varpi}^T\boldsymbol{\varpi} - c_2\boldsymbol{\varpi}^T\mathrm{sig}^c(\boldsymbol{\varpi}) \end{aligned} \tag{44}$$

Then using Lemma 1, (44) becomes

$$\begin{aligned} \dot{V} \le& -(k_1 - 1/2)\boldsymbol{S}^T\boldsymbol{S} - k_3(\boldsymbol{S}^T\boldsymbol{S})^{\frac{1+c}{2}} - c_2(\boldsymbol{\varpi}^T\boldsymbol{\varpi})^{\frac{1+c}{2}} \\ & -(c_1 - 1/2 - 1/2k_4^2)\boldsymbol{\varpi}^T\boldsymbol{\varpi} + 3\varrho \\ \le& -\mu_1 V - \mu_2 V^{\frac{1+c}{2}} + 3\varrho \end{aligned} \tag{45}$$

where μ_1=min$\{k_1 - 1/2, c_1 - 1/2 - 1/2k_4^2\}$, $\mu_2 = \min\{k_3, c_2\}$.

Consider the following two cases:

Case 1. If $\mu_1 V \ge 3\varrho$, then we have

$$\dot{V} \le -\mu_2 V^{\frac{1+c}{2}} \le 0 \tag{46}$$

Then from Lemma 3, it can be derived that the Lyapunov function V will satisfy $V \le 3\varrho/\mu_1$ in finite time.

Case 2. If $\mu_2 V^{\frac{1+c}{2}} \ge 3\varrho$, then we can get

$$\dot{V} \le -\mu_1 V \tag{47}$$

Similarly, Lyapunov function V satisfies the condition $V \le (3\varrho/\mu_2)^{\frac{1}{1+c}}$ in finite time. To incorporate the two cases, one can deduce that the sliding-mode surface $\boldsymbol{S}$ will converge to the following region

$$\|\boldsymbol{S}\| \le \min\{\sqrt{6\varrho/\mu_1}, \sqrt{2}(3\varrho/\mu_2)^{\frac{1}{1+c}}\} \triangleq \Delta \tag{48}$$

in finite time. On the other hand, we know that V is a radially unbounded Lyapunov function, and if the constant ϱ defined in the robust term satisfies $3\varrho \le \mu_1\hbar V$ with $\hbar \in (0, 1)$, then from (45) we can obtain

$$\dot{V} \ +\mu_1(1-\hbar)V + \mu_2 V^{\frac{1+c}{2}} \le 0 \tag{49}$$

Hence, using Lemma 2, upper bound of the convergence time can be estimated as

$$T \le \frac{2}{\mu_1(1-c)(1-\hbar)}\ln\frac{\mu_1(1-\hbar)V^{\frac{1-c}{2}}(0) + \mu_2}{\mu_2} \tag{50}$$

Moreover, consider the convergence region in (48) can be made enough small by choosing appropriate parameters of the observer. Hence, it can be concluded that the designed sliding-mode manifold can be driven to the bounded region in finite time. According to Theorem 1, the defined error variables given in (17) are finite-time stabilized in a small region including the zero point.

Denote $\boldsymbol{\upsilon}_e = [\upsilon_{1e}, \upsilon_{2e}, \upsilon_{3e}]^T$, $\boldsymbol{K}_1 = \mathrm{diag}[k_{11}, k_{12}, k_{13}]$, and then we have $S_i = \upsilon_{ie} + k_{1i}\xi_{ie}$, $i = 1, 2, 3$. If $\|\boldsymbol{S}\| \le \Delta$ holds in finite time, we have $|S_i| \le \Delta$. Then boundedness of υ_{ie} and ξ_{ie} can be proved by using the backstepping. If $|\upsilon_{ie}| \ge \Delta$, one can obtain

$$(1 - S_i/\upsilon_{ie})\upsilon_{ie} + k_{1i}\xi_{ie} = 0 \tag{51}$$

where $|S_i\upsilon_{ie}| \le 1$, and $|\xi_{ie}| \le \Delta k_{1i}$ is certainly established. Then we can get $|\upsilon_{ie}| \le |S_i| + k_{1i}|\xi_{ie}| \le 2\Delta$, and meanwhile, if $|\upsilon_{ie}| \le \Delta$ holds, we have $|\xi_{ie}| \le 2\Delta k_{1i}$, $i = 1, 2, 3$. Hence, finite-time stability of the closed-loop system motivated by the proposed control law has been proved.

Remark 5: In the task of attitude tracking, the CMG-based vehicle is assumed to move at a low speed to testify the

TABLE 1. Control parameters for the proposed controller.

Control terms	Parameter values
FTCESO	$\gamma_1 = 10$, $\gamma_2 = 0.05$, $\gamma_3 = 100$, $\gamma_4 = 1$, $\alpha_1 = 0.9$, $\lambda_1 = 10$, $\lambda_2 = 0.02$
SMC method	$\boldsymbol{K}_1 = 1.5\boldsymbol{I}_3$, $k_1 = 1.5$, $k_2 = 0.05$, $k_3 = 2$, $k_4 = 0.1$, $c = 0.5$
Anti-windup compensator	$c_1 = 0.7$, $c_2 = 0.7$, $\varpi = 0.001$
Robust term	$\sigma = 0.1$, =0.01
Feedback gain	$\lambda = 1$

capability of attitude control in a narrow space, which means that the control force τ_u will be chosen smaller.

Remark 6: For the proposed control law in (25), fast convergence of the reaching law may cause chattering to damage the system in a short time, and therefore k_2 needs to be smaller. The observer can be utilized to estimate and compensate for the system uncertainties to improve the control precision and reduce the chattering. In addition, the switch function is designed to allievate the switch gain of the control system, when the trajectory converges to the desired value in a finite time.

IV. NUMERICAL RESULTS

In this section, numerical simulations are performed for the attitude tracking control of the CMG-based AUV to validate the performance of the designed FTCESO-based sliding mode controller and the steering law for the CMG system.

In the simulation, accurate modeling parameters can refer to [47], which can be found in [34]. Specially, nominal parameters will simultaneously decrease 20% to the actual model. Meanwhile, two case studies are conducted to demonstrate the reliability of the designed controller, and in all simulations, the control force is chosen as $\tau_u = 2$ N, the CMG-based underwater vehicle moves with the initial position $\boldsymbol{\eta}_1(0) = \boldsymbol{0} \in \mathbb{R}^3$, attitude $\boldsymbol{q}(0) = [0, 0, 0, 1]^T$, linear velocity $\boldsymbol{\upsilon}_1(0) = \boldsymbol{0} \in \mathbb{R}^3$ and angular velocity $\boldsymbol{\upsilon}_2(0) = \boldsymbol{0} \in \mathbb{R}^3$. In addition, upper bounds of the supposed control input are selected as $\bar{\tau}_\kappa = 100\ N$ m, $\kappa \in \Omega$.

Table 1 presents the same control parameters for the two cases to demonstrate the effectiveness and reliability of the designed control scheme.

A. CASE STUDY 1

In this case, we consider the initial desired attitude $\boldsymbol{q}_d(0) = [0.3, 0.2, 0.5, -0.7874]^T$ with the angular velocity $\boldsymbol{\upsilon}_d = [0.1\sin(0.2t), 0.2\sin(0.3t), 0.3\sin(0.4t)]^T$ rad/s. In addition, the external disturbance vector $\boldsymbol{d}$ is chosen as $\boldsymbol{d} = [\sin(0.1t), \sin(0.2t), \sin(0.3t)]^T$.

As depicted in Fig. 3 and Fig. 4, precise attitude tracking control for the CMG-based AUV can be achieved with the employment of the proposed controller in the presence of the lumped disturbances including parameter uncertainties, time-varying external disturbances and input saturation. Also, the convergence time can be viewed in a short time for

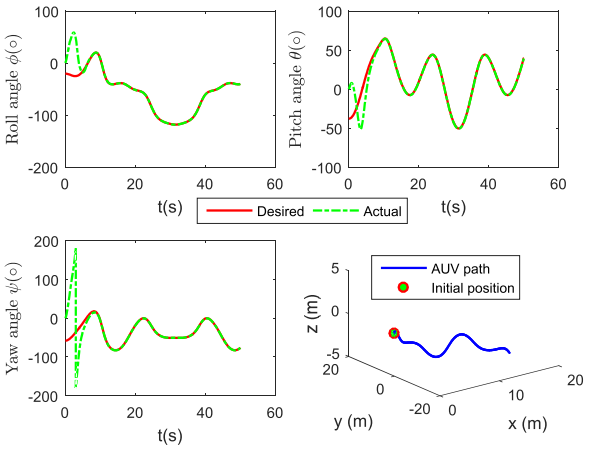

FIGURE 3. Tracking response of the attitude and its position variation.

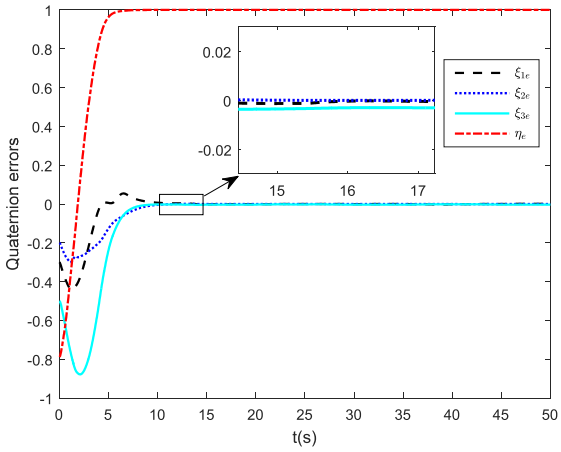

FIGURE 4. Error curves of the attitude quaternion.

obtaining the acceptable attitude control errors. As a consequence, the position variations presented in Fig. 3 indicate that this vehicle can perform the attitude control in a narrow space with a small constant force in the surge direction. In the initial stage, major changes of attitude curves can be partly to blame for the transformed torque error.

Meanwhile, Fig. 5 shows that the error of roll angular velocity varies a lot in the first 10 seconds compared with the other angular velocities in pitch and yaw directions. In fact, from Fig. 6 and Fig. 7, it can also be observed that time response curves of the sliding-mode surface and its estimation error based the FTCESO are with a large variation in the initial stage, especially evident in their first component. Due to the fact that the roll motion of an AUV is vulnerable to the hydrodynamics and external disturbances. It is used to conclude that roll motion control plays an important role in the initial process of tracking the desired attitude.

As a matter of fact, most AUVs are operating at a low speed or equipped with special roll actuators to do the roll motion to guarantee a proper stability margin in the roll direction.

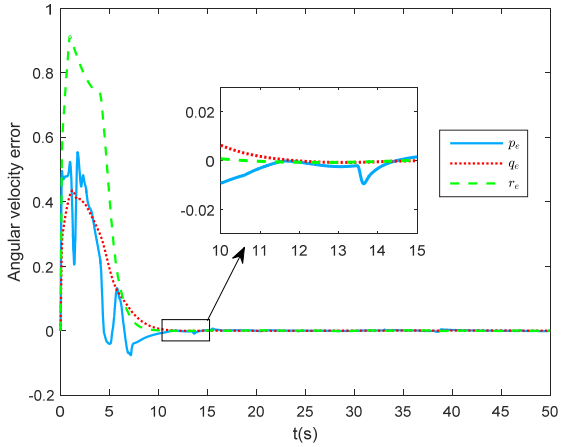

FIGURE 5. Error curves of angular velocity.

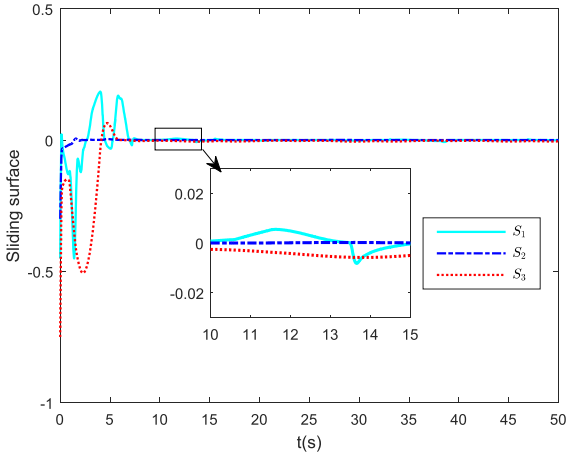

FIGURE 6. Time histories of the sliding-mode surface.

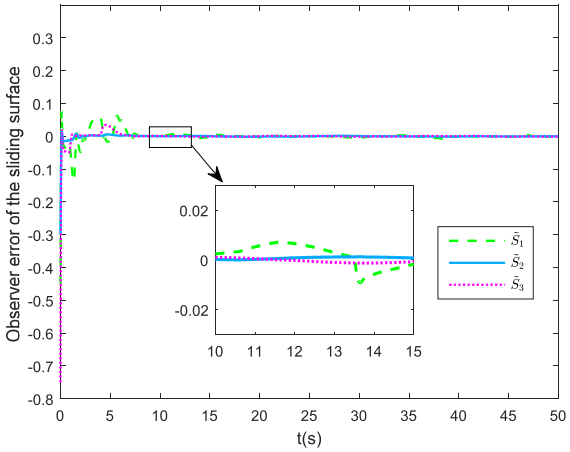

FIGURE 7. Error curves of sliding-mode surface estimation.

In this paper, internal CMG system is considered to generate the moment to control the attitude in three-axis, and thus effects of the coupling dynamics are taken into the controller design to reduce the interaction in the attitude adjusting.

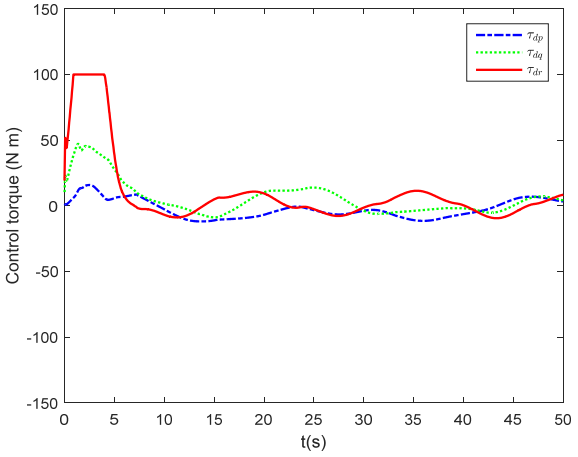

FIGURE 8. Time histories of the designed control torque.

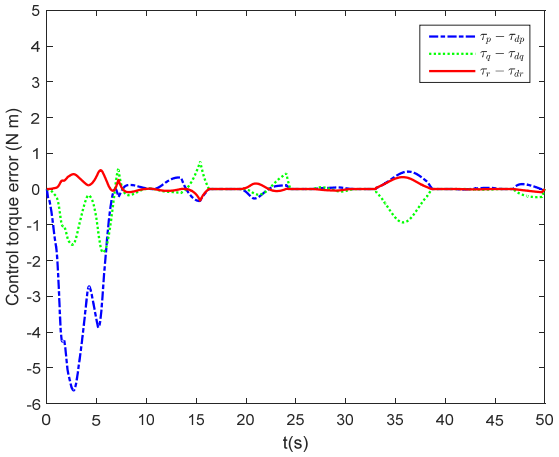

FIGURE 9. Error curves of the control torque.

Hence, initial velocity error of the roll direction is deemed acceptable in the simulation results.

Figure 8 and Fig. 9 give the time histories of the desired control moment and actual output torque error during the transformation, respectively. As presented in Fig. 8, the control system is suffered from the input saturation in yaw direction. Meanwhile, it can be found in Fig. 9 that output torque generated from the CMG cluster cannot be thought to be equivalent to the designed torque for the attitude tracking control system, which means that the closed-loop system should address the internal torque disturbances to accomplish the tracking mission.

In addition, time response curve of the gimbal rate is provided in Fig. 10. It can be deduced that the gimbal rate is reasonable to output the torque with the consideration of the physical limitation. In addition, reference profiles of the CMG cluster indicate that the attitude control device is competent to generate real-time control torque for the attitude tracking with the proposed control framework. The transformed torque error may not be neglected though the CMG

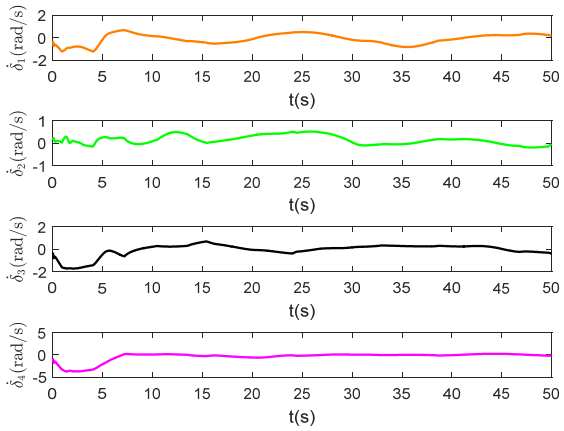

FIGURE 10. Time histories of the gimbal rate.

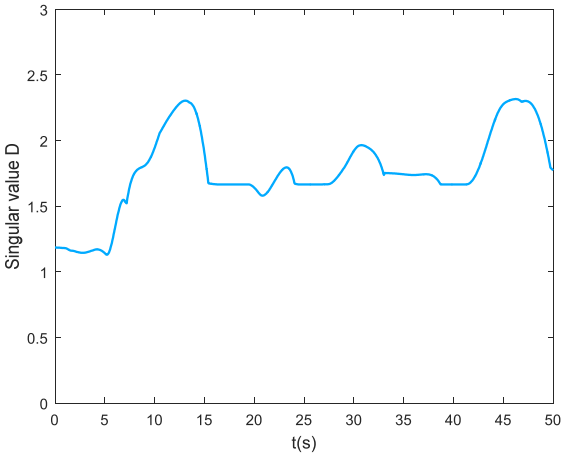

FIGURE 11. Time histories of the singular value.

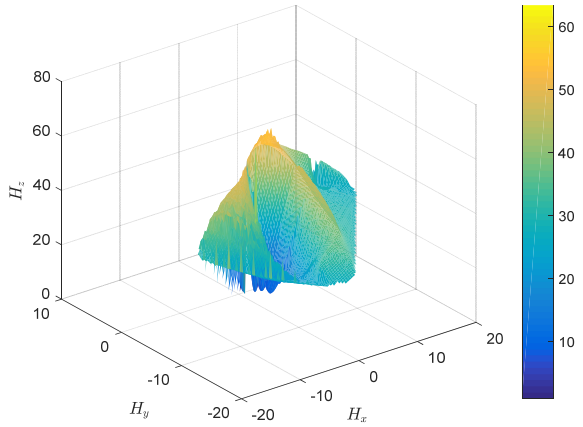

FIGURE 12. Angular momentum surface versus time.

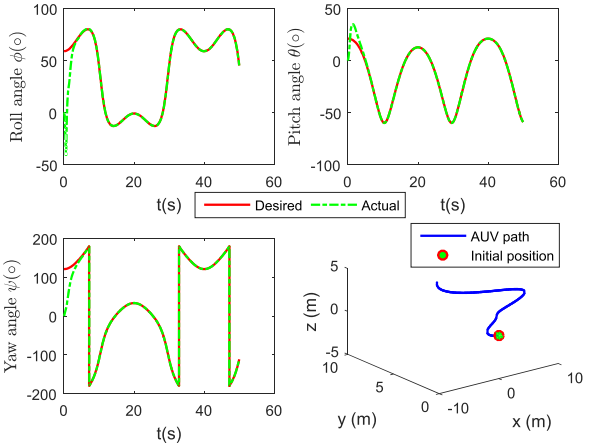

FIGURE 13. Tracking response of the attitude and its position variation.

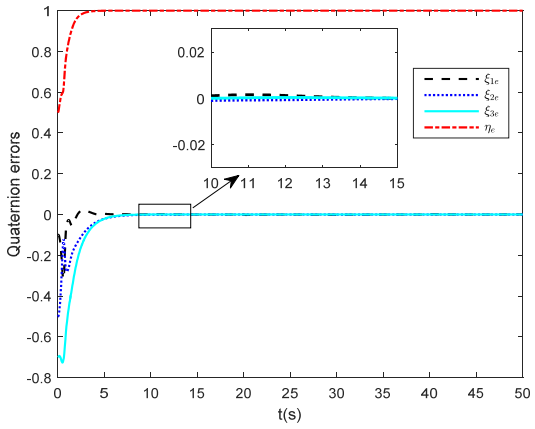

FIGURE 14. Error curves of the attitude quaternion.

system is controlled by the proposed steering law to output the torque without error in theory.

Meanwhile, the index of the singular state in Fig. 11 shows that the CMG system is working normally with the aid of the constrained steering law. What's more, angular momentum surface can be visualized in Fig. 12 to show its variation during the task of attitude tracking control.

B. CASE STUDY 2

To further inspect the disturbance rejection of the designed control strategy, persistent disturbances of the inertia matrix are taken into consideration, which means that the actual inertia matrix of the CMG-based AUV is defined to be $\boldsymbol{I} = \boldsymbol{I}_0 + \Delta\boldsymbol{I} + \boldsymbol{I}_t$, where $\boldsymbol{I}_t$ is given by $\boldsymbol{I}_t = \text{diag}[0.1\sin(0.1t), 0.2\sin(0.2t), 0.3\sin(0.3t)]$; besides, the disturbance vector $\boldsymbol{d}$ is chosen as $\boldsymbol{d} = 0.1\text{sig}^0(\boldsymbol{v}_2) + \boldsymbol{d}_t$, where $\boldsymbol{d}_t = [\sin(0.1t), 2\sin(0.2t), 3\sin(0.3t)]^T$. Meanwhile, we consider the initial desired attitude in this case is $\boldsymbol{q}_d(0) = [0.1, 0.5, 0.7, 0.5]^T$ with the desired angular velocity $\boldsymbol{v}_d = [0.1\sin(\pi t 20), 0.2\sin(\pi t 20), 0.3\sin(\pi t 20)]^T$ rad/s.

In this case, path of the vehicle is a spiral line which can be shown in Fig. 13. Also, the results in Fig. 13 and Fig. 14 manifest that the CMG-based AUV can achieve the task of precise attitude control using the proposed controller in spite of the added internal disturbances and non-differentiable external disturbances.

As illustrated in Figs. 15-17, initial errors of the angular velocity, the sliding surface and its estimation in the roll

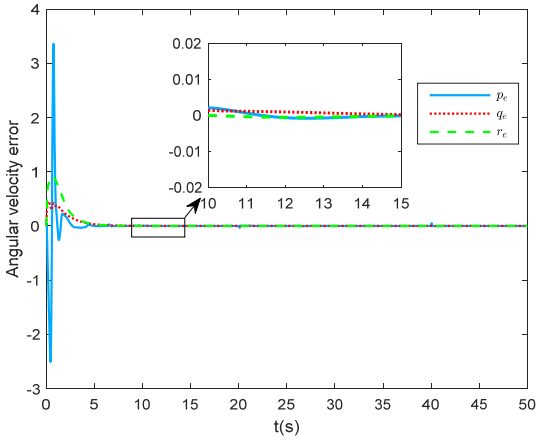

FIGURE 15. Error curves of angular velocity.

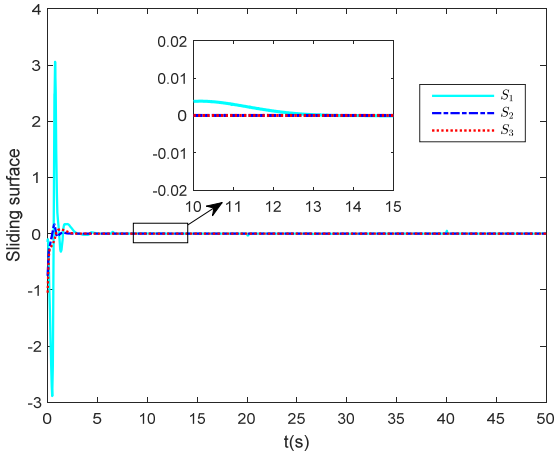

FIGURE 16. Time histories of the sliding-mode surface.

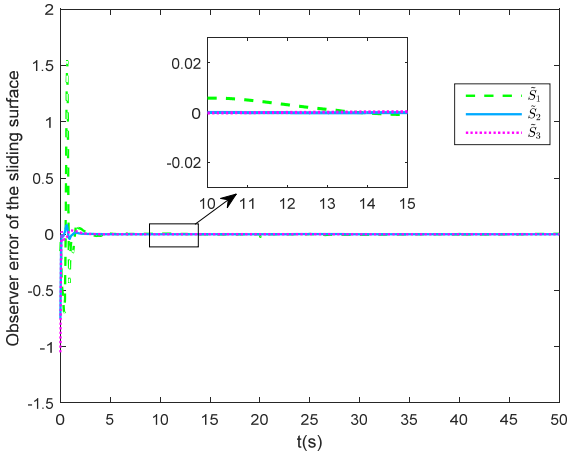

FIGURE 17. Error curves of sliding-mode surface estimation.

direction are significantly more than their relative profiles in other two directions. In in Figs. 15-17, the peak and valley appear at the initial stage. From the aforementioned analyses, we know that roll motion of an AUV is sensitive

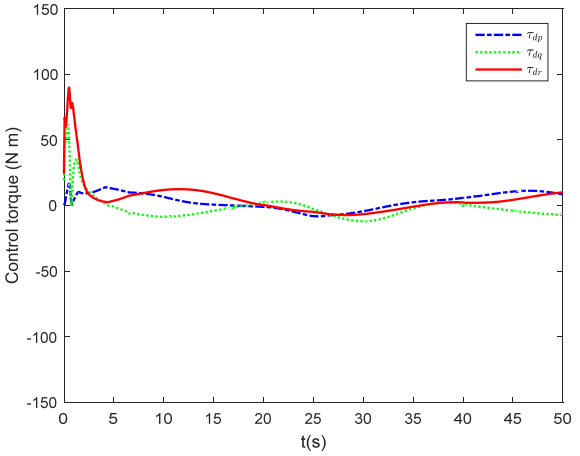

FIGURE 18. Time histories of the designed control torque.

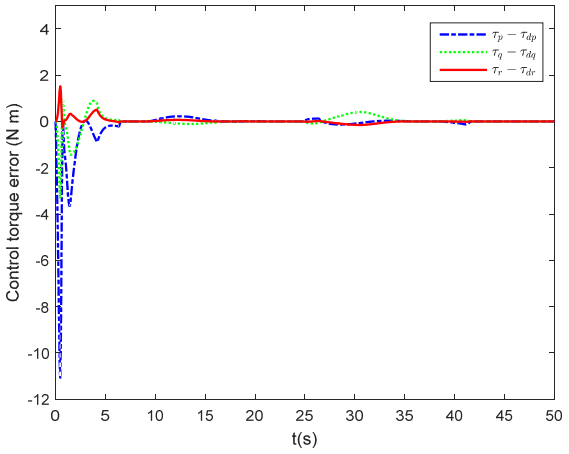

FIGURE 19. Error curves of the control torque.

to the hydrodynamic force and torque, and this may cause the undesirable behavior in the predefined attitude tracking mission. On the other hand, the reason for differences in the amplitude and frequency should contain the designed control parameters, lumped uncertainties and initial posture in tracking the specified attitude trajectory.

Fig. 18 and Fig. 19 display the response curves of the designed control moment and its transformed error by means of the actuator kinematics, respectively. In this case, the vehicle is free from the input saturation problem to achieve the tracking mission. Meanwhile, the transformed torque error converges to zero rather than the continuing disturbance acting on the first case. But the curves of the control torque variation are smooth to show the robustness properties of the tracking control framework to reject both internal and external uncertainties.

Similarly, we provide response curves of the gimbal rate and singular value of the pyramid-array CMG cluster in Figs. 20-21, respectively. It reveals that the singularity problem of the CMG system would never occur with the aid

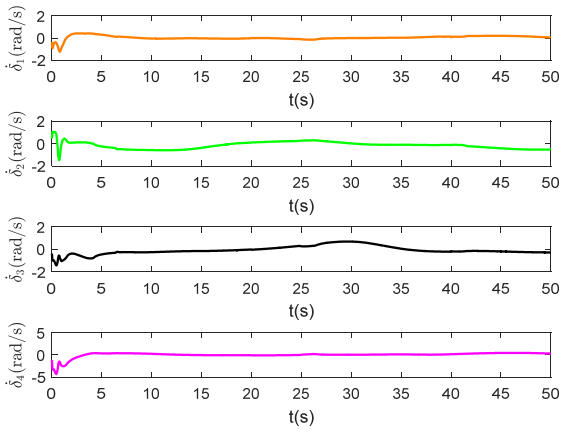

FIGURE 20. Time histories of the gimbal rate.

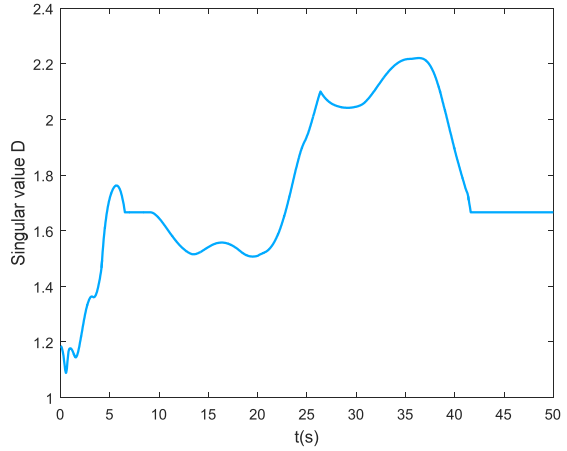

FIGURE 21. Time histories of the singular value.

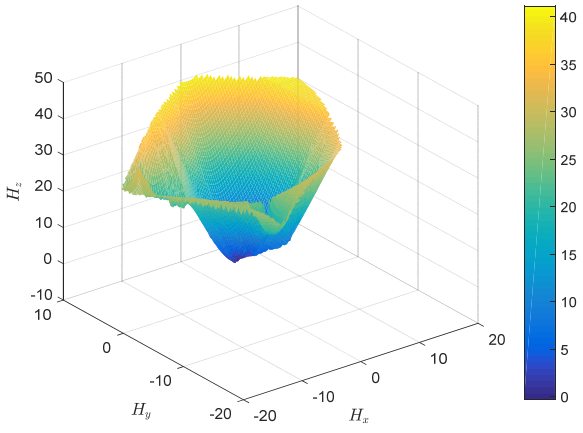

FIGURE 22. Angular momentum surface versus time.

of constrained steering law in the restricted workspace. Also, visualization of the angular momentum surface versus time can be found in Fig. 23. In the above two cases, it's convinced that the constrained workspace possesses the maximum size as the original unrestricted system in z direction, and almost one-third size in the x (or y) direction [45].

According to various simulation results in the two cases, it can be concluded that the proposed control framework can guarantee its robustness and tracking performance against the aggregated nonlinearities, which may include inaccurate model parameters, undesirable internal torque perturbations, time-varying external disturbances and input saturation. Meanwhile, finite-time stability of the closed-loop system can be achieved to show its superiority. In addition, other simulation results confirm the tracking performance of the control law, which are omitted here to save the space.

V. COMPARISION WITH OTHER RESULTS

To highlight the novelty of the obtained results in this paper, some descriptions are presented as follows.

(1) To the best of the author's knowledge, this paper first investigates the problem of three-axis attitude tracking control for a CMG-based AUV in the presence of the lumped disturbances, which include the parametric uncertainties, coupling dynamic characteristics, input saturation, internal and external disturbances. This is different from the previous studies, which contain the position and attitude tracking control problem solved for full-actuated AUV without taking the assumed uncertainties into account [17], [18], single-direction attitude control for the AUVs in [11], [12], and the unrestricted attitude control for a Zero-G class CMG-actuated AUV in [16] without considering the external disturbances and input saturation.

(2) Compared with the traditional attitude control for the unmanned aerial vehicle (UAV) or spacecraft, more motion constraints are considered and resolved in the control object of this paper, i.e., the coupling dynamic effects generated from the AUV's translation motion and rotational motion, and dynamic behavior of the attitude control device. Hence, these results cannot be directly extended to the attitude control for the CMG-based AUV with the assumed uncertainties considered.

(3) Different from the attitude control for UAV or spacecraft using the approach of TSMC [28], [29], finite-time stability of the attitude control system in this paper is achieved by a linear SMC method in conjunction with the FTCESO, which simplifies the controller design and avoid the singularity problem in TSCM method. In addition, anti-windup compensator is employed to release the burden of the observer, and a switch function is designed to display the power of the robust controller and the constant-rate reaching law.

However, several problems should be considered in the future work to improve the designed control strategy for the attitude control for the CMG-based underwater vehicle.

(4) Actuator faults and dead-zone nonlinearities are not taken into the development of the proposed controller.

(5) Some signals relative to the roll direction vary widely in a short time during the initial period, and thus a

parameter optimization mechanism may need to be considered to tackle this issue and to keep a balance between the convergence time and system reliability.

Alternatively, future work can test the attitude control ability of a CMG-based AUV prototype using the proposed control scheme in open water.

VI. CONCLUSION

This paper investigated the problem of three-axis attitude tracking control of a CMG-based AUV, with the existence of parameter perturbation, unknown external disturbances and input saturation nonlinearity. In order to guarantee finite-time stability of the designed control framework, a FTCESO is taken here to estimate the variation of a linear sliding mode surface, and then the anti-windup compensator is employed to address the input saturation in order to relieve the stress of the observer and enhance its tolerance for the internal torque errors. In addition, the robust term and constant-reaching law are separated by a switch function to show their abilities to compensate for the observer error. Finite-time stability of the attitude tracking system is guaranteed by the Lyapunov theory. Finally, two studies implemented in the simulations validate the performance and effectiveness of the designed control scheme. Future work can start from the fault-tolerant attitude control for AUVs, and the steering logic for CMGs should be improved to promote its adaptability in different situations.

REFERENCES

[1] L. Lapierre, D. Soetanto, and A. Pascoal, "Nonlinear path following with applications to the control of autonomous underwater vehicles," in *Proc. 42nd IEEE CDC*, Maui, HI, USA, Dec. 2003, pp. 1256–1261.

[2] L. Lapierre and B. Jouvencel, "Robust nonlinear path-following control of an AUV," *IEEE J. Ocean. Eng.*, vol. 33, no. 2, pp. 89–102, Apr. 2008.

[3] K. Shojaei and M. Dolatshahi, "Line-of-sight target tracking control of underactuated autonomous underwater vehicles," *Ocean Eng.*, vol. 133, pp. 244–252, Mar. 2017.

[4] G. Ferri, A. Munafò, and K. D. Lepage, "An autonomous underwater vehicle data-driven control strategy for target tracking," *IEEE J. Ocean. Eng.*, vol. 43, no. 2, pp. 323–343, Apr. 2018.

[5] C. Yu, X. Xiang, Q. Zhang, and G. Xu, "Adaptive fuzzy trajectory tracking control of an under-actuated autonomous underwater vehicle subject to actuator saturation," *Int. J. Fuzzy Syst.*, vol. 20, no. 1, pp. 269–279, Jan. 2018.

[6] X. Xiang, B. Jouvencel, and O. Parodi, "Coordinated formation control of multiple autonomous underwater vehicles for pipeline inspection," *Int. J. Adv. Robotic Syst.*, vol. 7, no. 1, pp. 75–84, Mar. 2010.

[7] B. Das, B. Subudhi, and B. B. Pati, "Cooperative formation control of autonomous underwater vehicles: An overview," *Int. J. Automat. Comput.*, vol. 13, no. 3, pp. 199–225, Jun. 2016.

[8] O.-E. Fjellstad and T. I. Fossen, "Position and attitude tracking of AUV's: A quaternion feedback approach," *IEEE J. Ocean. Eng.*, vol. 19, no. 4, pp. 512–518, Oct. 1994.

[9] G. Antonelli, S. Chiaverini, N. Sarkar, and M. West, "Adaptive control of an autonomous underwater vehicle: Experimental results on ODIN," *IEEE Trans. Control Syst. Technol.*, vol. 9, no. 5, pp. 756–765, Sep. 2001.

[10] V. Arrichiello, G. Bartolini, A. Pisano, E. Punta, E. Usai, and T. Zolezzi, "Attitude and position tracking of autonomous 6 d.o.f. vehicles with mono-directional actuators," in *Proc. 14th VSS*, Nanjing, China, 2016, pp. 80–85.

[11] B. Li and T.-C. Su, "Heading autopilot of autonomous underwater vehicles with internal moving mass," *J. Comput. Nonlinear Dyn.*, vol. 12, no. 2, pp. 021003-1–0201003-7, Mar. 2017.

[12] R. Cui, X. Zhang, and D. Cui, "Adaptive sliding-mode attitude control for autonomous underwater vehicles with input nonlinearities," *Ocean Eng.*, vol. 123, pp. 45–54, Sep. 2016.

[13] Y. Jia and A. K. Misra, "Robust trajectory tracking control of a dual-arm space robot actuated by control moment gyroscopes," *Acta Astronautica*, vol. 137, pp. 287–301, Aug. 2017.

[14] B. Thornton, T. Ura, and Y. Nose, "Wind-up AUVs: Combined energy storage and attitude control using control moment gyros," in *Proc. Oceans Conf.*, Vancouver, BC, Canada, 2007, pp. 1–9.

[15] B. Thornton, T. Ura, Y. Nose, and S. Turnock, "Internal actuation of underwater robots using control moment gyros," in *Proc. Eur. Oceans Conf.*, Brest, France, 2005, pp. 591–598.

[16] B. Thornton, T. Ura, Y. Nose, and S. Turnock, "Zero-G class underwater robots: Unrestricted attitude control using control moment gyros," *IEEE J. Ocean. Eng.*, vol. 32, no. 3, pp. 565–583, Jul. 2007.

[17] K. Y. Pettersen and O. Egeland, "Time-varying exponential stabilization of the position and attitude of an underactuated autonomous underwater vehicle," *IEEE Trans. Autom. Control*, vol. 44, no. 1, pp. 112–115, Jan. 1999.

[18] G. Bartolini and A. Pisano, "Black-box position and attitude tracking for underwater vehicles by second-order sliding-mode technique," *Int. J. Robust Nonlinear Control*, vol. 20, no. 14, pp. 1594–1609, Sep. 2010.

[19] K. D. Young, V. I. Utkin, and U. Ozzguner, "A control engineer's guide to sliding mode control," *IEEE Trans. Control Syst. Technol.*, vol. 7, no. 3, pp. 328–342, May 1999.

[20] L. Zhou, Z. Che, and C. Yang, "Disturbance observer-based integral sliding mode control for singularly perturbed systems with mismatched disturbances," *IEEE Access*, vol. 6, pp. 9854–9861, Feb. 2018.

[21] M. He and J. He, "Extended state observer-based robust backstepping sliding mode control for a small-size helicopter," *IEEE Access*, vol. 6, pp. 33480–33488 Jun. 2018.

[22] B. Das, B. Subudhi, and B. B. Pati, "Adaptive sliding mode formation control of multiple underwater robots," *Arch. Control Sci.*, vol. 24, no. 4, pp. 515–543, Dec. 2014.

[23] X. Guo, W. Yan, and R. Cui, "Neural network-based nonlinear sliding-mode control for an AUV without velocity measurements," *Int. J. Control*, vol. 1, pp. 677–692, Aug. 2017.

[24] W. M. Bessa, M. S. Dutra, and E. Kreuzer, "Depth control of remotely operated underwater vehicles using an adaptive fuzzy sliding mode controller," *Robot. Auton. Syst.*, vol. 56, no. 8, pp. 670–677, Aug. 2008.

[25] T. Elmokadema, M. Zribia, and K. Youcef-Toumi, "Terminal sliding mode control for the trajectory tracking of underactuated autonomous underwater vehicles," *Ocean Eng.*, vol. 129, pp. 613–625, Jan. 2017.

[26] R. Cui, L. Chen, C. Yang, and M. Chen, "Extended state observer-based integral sliding mode control for an underwater robot with unknown disturbances and uncertain nonlinearities," *IEEE Trans. Ind. Electron.*, vol. 64, no. 8, pp. 6785–6795, Aug. 2017.

[27] Y. Xia, Z. Zhu, M. Fu, and S. Wang, "Attitude tracking of rigid spacecraft with bounded disturbances," *IEEE Trans. Ind. Electron.*, vol. 58, no. 2, pp. 647–659, Feb. 2011.

[28] Z. Han, K. Zhang, T. Yang, and M. Zhang, "Spacecraft fault-tolerant control using adaptive non-singular fast terminal sliding mode," *IET Control Theory Appl.*, vol. 10, no. 16, pp. 1991–1999, Oct. 2016.

[29] H. Gui and G. Vukovich, "Adaptive integral sliding mode control for spacecraft attitude tracking with actuator uncertainty," *J. Franklin Inst.*, vol. 352, no. 12, pp. 5832–5852, Dec. 2015.

[30] X. Ma, F. Sun, H. Li, and B. He, "Attitude control of rigid body with inertia uncertainty and saturation input," *Tsinghua Sci. Technol.*, vol. 22, no. 1, pp. 83–91, Feb. 2017.

[31] M. Chen, Q.-X. Wu, and R.-X. Cui, "Terminal sliding mode tracking control for a class of SISO uncertain nonlinear systems," *ISA Trans.*, vol. 52, no. 2, pp. 198–206, Mar. 2013.

[32] R. Xu, G. Tang, D. Xie, D. Huang, and L. Jun, "Underactuated tracking control of underwater vehicles using control moment gyros," *Int. J. Adv. Robotic Syst.*, vol. 15, no. 1, pp. 1–8, Jan./Feb. 2018.

[33] R. Xu, G. Tang, D. Xie, Z. Liu, and J. Qian, "Dynamic simulation modeling and analysis of an internal CMG-actuated underwater vehicle," in *Proc. IEEE ICASI*, Chiba, Japan, Apr. 2018, pp. 27–30.

[34] R. Xu, G. Tang, L. Han, and D. Xie, "Trajectory tracking control for a CMG-based underwater vehicle with input saturation in 3D space," *Ocean Eng.*, vol. 173, pp. 587–598, Feb. 2019.

[35] Y. Zuo and L. Tie, "A new class of finite-time nonlinear consensus protocols for multi-agent systems," *Int. J. Control*, vol. 87, no. 2, pp. 363–370, Feb. 2014.

[36] S. Yu, X. Yu, B. Shirinzadeh, and Z. Man, "Continuous finite-time control for robotic manipulators with terminal sliding mode," *Automatica*, vol. 41, no. 11, pp. 1957–1964, Nov. 2005.

[37] M. M. Polycarpou, "Stable adaptive neural control scheme for nonlinear systems," *IEEE Trans. Autom. Control*, vol. 41, no. 3, pp. 447–451, Mar. 1996.
[38] T. I. Fossen, *Guidance and Control of Ocean Vehicles*. London, U.K.: Wiley, 1994, pp. 6–18.
[39] H. Kurokawa, "Survey of theory and steering laws of single-gimbal control moment gyros," *J. Guid. Control Dyn.*, vol. 30, no. 5, pp. 1331–1340, 2007.
[40] B. Wie, C. Heiberg, and D. Bailey, "Singularity robust steering logic for redundant single-gimbal control moment gyros," *J. Guid. Control Dyn.*, vol. 24, no. 5, pp. 865–872, Sep./Oct. 2001.
[41] S. Xiong, W. Wang, X. Liu, Z. Chen, and Wang, "A novel extended state observer," *ISA Trans.*, vol. 58, pp. 309–317, Sep. 2015.
[42] Z.-G. Hou, A.-M. Zou, L. Cheng, and M. Tan, "Adaptive control of an electrically driven nonholonomic mobile robot via backstepping and fuzzy approach," *IEEE Trans. Control Syst. Technol.*, vol. 17, no. 4, pp. 803–815, Jul. 2009.
[43] S. Lee and S. Jung, "Experimental verification of singularity-robust torque control for a 1.2-Nm–5-Hz SGCMG," *IEEE Trans. Ind. Electron.*, vol. 65, no. 6, pp. 4871–4879, Jun. 2018.
[44] J. Guo, B. Wu, Y. Geng, X. Kong, and Z. Hou, "Rapid SGCMGs singularity-escape steering law in gimbal angle space," *IEEE Trans. Ind. Electron.*, vol. 54, no. 5, pp. 2509–2525, Oct. 2018.
[45] H. Kurokawa, "Constrained steering law of pyramid-type control moment gyros and ground tests," *J. Guid. Control Dyn.*, vol. 20, no. 3, pp. 445–449, 1997.
[46] R. Cristi, J. Burl, and N. Russo, "Adaptive quaternion feedback regulation for eigenaxis rotations," *J. Guid. Control Dyn.*, vol. 17, no. 6, pp. 1287–1291, Nov./Dec. 1994.
[47] T. Prestero, "Verification of a six-degree of freedom simulation model for the REMUS autonomous underwater vehicle, REMUS (autonomous underwater vehicle)," M.S. thesis, Massachusetts Inst. Technol., and Woods Hole Oceanographic Inst., Boston, MA, USA, 2001.

Authors' photographs and biographies not available at the time of publication.